Nuclear Materials and Energy 33 (2022) 101256

Contents lists available at ScienceDirect

Nuclear Materials and Energy

journal homepage: www.elsevier.com/locate/nme

Comparison of the deuterium permeability of copper, CuCrZr, and Cu layers

A. Houben *, M. Rasiński, S. Brezinsek, Ch. Linsmeier

Forschungszentrum Jülich GmbH, Institut für Energie- und Klimaforschung – Plasmaphysik, Partner of the Trilateral Euregio Cluster (TEC), 52425 Jülich, Germany

ARTICLE INFO

Keywords:
Gas-driven deuterium permeation
Cu and Cu layers
CuCrZr - ITER grade
Microstructure
Interface
Magnetron sputter deposition

ABSTRACT

In order to estimate the fuel loss in ITER and further future fusion devices, the deuterium permeation through different wall and structural materials are studied. In order to determine the effective permeability, gas-driven deuterium permeation measurements are performed on Cu and ITER grade CuCrZr. The obtained permeabilites for Cu and ITER grade CuCrZr are very similar and in agreement to literature values for Cu. For a better estimation for fusion reactor components, combined material samples are studied. Cu layers were applied on steel substrates by magnetron sputter deposition. With these studies, the influence of interfaces and microstructure on the hydrogen permeation is investigated. Our study reveals that in the case of Cu layered steel substrates the influence of the interface on the permeation flux is minor compared to the influence of the microstructure on the permeability. The Cu layer permeability is around one order of magnitude smaller than the Cu bulk permeability in the temperature range between 300°C and 550°C.

1. Introduction

The estimation of the hydrogen isotope permeation flux through fusion materials and components is required in order to estimate the fuel loss of a fusion device. Furthermore, this knowledge is helpful for the selection of materials and an improved design of components for future fusion devices [1].

Copper, Cu alloys and steels are foreseen as materials for the first wall components in ITER and future fusion devices [2,3]. The deuterium permeability of pure copper and the ITER grade (IG) Cu alloy CuCrZr-IG were measured by gas-driven permeation measurements and are compared to the 316L(N)-IG steel [4].

Since the sample thickness is limited to a few mm in a gas-driven permeation setup, it is not possible to measure a whole fusion component, which is about two to three orders of magnitude larger. Therefore, different combinations of fusion materials, which will be used in ITER and future fusion devices, are under study. Cu layers were deposited by magnetron sputtering on polished 316L(N)-IG substrates. In order to estimate the influence of the interface, three Cu layered substrates were fabricated, characterized and measured with three different Cu layer thicknesses between 490 nm and 1400 nm. With this, the layer bulk/interface ratio was varied in order to separate the influence of the layer microstructure and the influence of the interface on the permeability, as illustrated in Fig. 1.

Additional to the measurement of the deuterium permeability through the ITER materials, an overview of various influences on the permeation flux will be obtained by comparison of the permeability of the single materials and layered substrates. This knowledge will be used to determine which sample parameters and characteristics are important for a reliable estimation of the permeation flux through a fusion component.

2. Sample preparation

For the pure copper samples, commercial oxygen-free copper was used. The CuCrZr raw material was provided by F4E and the ITER Organization. The CuCrZr blocks were fabricated by Albaksan A.S. and have a composition of about 98.9% Cu, 0.85% Cr and 0.13% Zr according to the test certificate provided by the company. From the raw materials, disks with a diameter of 24 mm and a thickness of 0.5 mm were cut, grinded and polished on both sides. After the last polishing step with a 1 μm diamond suspension, a cleaning with an oxide polishing suspension was applied. The polishing procedure was adapted to the hardness of the material in order to obtain a mirror finished surface with no smear layer. The resulting thickness of the substrates after polishing procedure are around 0.3 mm. These samples are named Cu (bulk) and CuCrZr in the following.

For the Cu layered samples, polished 316L(N)-IG samples were used as substrates, please find details to the substrate in [4]. The sample plate of the magnetron device (PREVAC) was rotated during deposition process in order to obtain a homogeneous layer. A pure copper sputter target (99.999% Cu, Lesker) was used and an Ar plasma. Several samples were coated during one deposition process, which therefore are

* Corresponding author.
E-mail address: an.houben@fz-juelich.de (A. Houben).

https://doi.org/10.1016/j.nme.2022.101256
Received 24 June 2022; Received in revised form 29 August 2022; Accepted 14 September 2022
Available online 20 September 2022

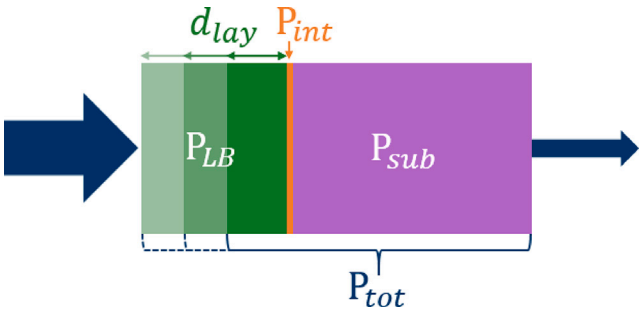

Fig. 1. Schematic illustration of the layer thickness variation. d_{lay} represents the layer thickness, P_{tot}, P_{sub}, P_{LB}, and P_{int} the permeability of the layered substrate, the substrate, the layer bulk, and the interface, respectively. The shown proportions do not correspond to the real thicknesses and are for illustration only.

identical in microstructure and thickness. The substrates were coated on one side only. The thickness of the layer was varied through the duration of the deposition of each process. Three deposition processes were carried out. The obtained layer thicknesses are 490 nm (named 316L_Cu_thin), 980 nm (named 316L_Cu_thick), and 1400 nm (named 316L_Cu_very_thick). In the following, the terms 'layered substrate' will be used for the complete sample system and 'Cu layer' for the single layer after deduction of the 316L substrate.

Before characterization and measurements, all samples were pre-annealed at the maximum applied temperature of 550°C for several hours in order to remove natural hydrogen and in order to obtain a stable sample condition.

3. Measurement methods

All sample surfaces were analyzed by scanning electron microscopy (SEM) with a Zeiss Crossbeam 540 after pre-annealing. For the Cu layered substrates, cross sections were created by focused ion beam (FIB) enabling a further characterization of the layer by SEM and the measurement of the layer thickness. All figures shown were recorded in SE mode. If needed, energy dispersive X-ray spectroscopy (EDX) measurements were used for elemental analysis. The EDX setup (Oxford X-Max 80) is attached to the SEM(FIB) device.

The gas-driven permeation measurements were performed in an in-house permeation setup. The sample separates two volumes, the low and high pressure volume. Before measurement, both volumes are evacuated to a base pressure of 10^{-9} mbar. After stabilizing the desired sample temperature, pure deuterium gas is inserted in the high pressure volume and the permeation flux in the low pressure volume is measured by a quadrupole mass spectrometer (Pfeiffer Vacuum). The mass spectrometer is calibrated by four D_2 calibration leaks (LACO Technologies) with fixed deuterium fluxes. The measurement cycles are identical for all samples and the measurement range of the sample temperature is between 300°C and 550°C ("up-measurement"). At each temperature step, the gas pressure is varied between 25 mbar and 800 mbar. In order to observe a possible change of sample during measurement (e.g. oxidation, change of microstructure), after the last temperature step of 550°C, the 500°C to 300°C measurements are repeated ("down-measurement"). If the up- and down-measurements corresponds to each other, the respective sample did not change during measurement. The precise thicknesses of the substrates or the layered substrates are measured by a micrometer screw after permeation measurement in order to avoid scratches on the surface before permeation measurement which could influence the permeation.

4. Data analysis

By measuring the permeation flux as a function of applied deuterium pressure and sample temperature, the process limiting regime and the permeability can be determined. In the diffusion limited regime, where the surface processes are fast in comparison to the diffusion process, the permeation flux is proportional to the square root of the applied pressure and dependent on the sample or layer thickness. If the permeation flux is linearly dependent on the applied pressure, the surface or interface processes limit the permeation process and the permeation flux is not dependent on the thickness of the sample or layer. In the diffusion limited regime, the permeability constant P_0 and the activation energy E_P can be obtained from the permeation flux J_P:

$$J_P = \frac{P_0\sqrt{p}}{d} e^{\frac{-E_P}{RT}} \tag{1}$$

wherein d is the thickness of the sample, R is the ideal gas constant and T the sample temperature. The obtained permeability $P = P_0 e^{\frac{-E_P}{RT}}$ is valid in the measured temperature and pressure range only.

For the layered substrates, the layer permeability P_{lay} was estimated by the permeability of the substrate P_{sub} and the permeability of the layered substrate P_{tot}:

$$P_{lay} = \frac{d_{lay}}{\frac{d_{tot}}{P_{tot}} - \frac{d_{sub}}{P_{sub}}} \tag{2}$$

wherein d_{tot}, d_{sub}, and d_{lay} are the thicknesses of the layered substrate, the substrate and the layer, respectively [5]. We want to point out that the layer permeability is an estimation after deduction of the substrate permeability from the total system permeability. With the assumption that P_{tot} scales with the thickness of the layer, the layer thickness is regarded in Eq. (2). Therefore, the layer permeability is only valid in the diffusion limited regime. It contains all effects which influence the permeability such as surface, interfaces, microstructure and further properties of the layer system. With the layer permeability, a substrate and layer thickness independent value is given with which a comparison of different layers is more reliable.

5. Results

The surfaces of the polished substrate samples Cu and CuCrZr were analyzed by SEM, see Fig. 2. No smear layer of the grinding procedure can be observed and the microstructure is clearly visible. The Cu substrate shows grains of around 50 µm size and voids. The CuCrZr sample shows precipitates with an accumulation around the grain boundaries. An EDX analysis of this surface confirmed that the matrix is pure Cu, whereas the precipitates are Cr. A signal from Zr cannot be detected by EDX due to the small amount of Zr in the alloy. However, we assume that the Zr forms CuZr phases [6].

The surface of the Cu layered substrates were analyzed by SEM, see Fig. 3 left side. On the right side of Fig. 3 the SEM figures of the cross sections through the layers prepared by FIB are shown. The surface structure of the samples 316L_Cu_thin (Fig. 3a) and 316L_Cu_very_thick (Fig. 3c) are similar, whereas the surface of 316L_Cu_thick (Fig. 3b) looks rougher and scratchy. In the cross section of the 316L_Cu_thick it is observe that these scratches are on the top of the surface only. The reason for the development of these surface characteristics, which were created during deposition, is unclear, but the influence on the permeation is assumed to be minor. The microstructure of all three layers is similar. The grain size is around two orders of magnitude smaller as in the bulk Cu substrate and no voids, pores, intermediate phases or precipitates can be observed. The layers are homogeneous and the thickness was measured on these cross sections: 490 nm (316L_Cu_thin), 980 nm (316L_Cu_thick), and 1400 nm (316L_Cu_very_thick).

The permeation flux versus the applied deuterium pressure and the respective Arrhenius plot are shown for the 316L_Cu_thick sample in Fig. 4 as an example for the data analysis. From Fig. 4a the exponent of the pressure dependence was extracted for each temperature step and a mean value is given in Table 1. The permeability was obtained from the Arrhenius plot (Fig. 4b) for each pressure step, and the mean values for the permeation constant P_0 and the activation energy E_P are

Table 1
The results obtained from temperature and pressure dependent permeation measurements: pressure dependence p^x, permeation constant P_0, and activation energy E_P. The values for the 316L substrate are taken from [4].

Sample	p^x	P_0 $\left[\frac{\text{mol}}{\text{ms}\sqrt{\text{mbar}}}\right]$	E_P $\left[\frac{\text{kJ}}{\text{mol}}\right]$
Cu	0.55	$3(2)\cdot10^{-6}$	77(2)
CuCrZr	0.55	$6(2)\cdot10^{-6}$	79(1)
316L_Cu_thin	0.6	$4(2)\cdot10^{-7}$	55(2)
316L_Cu_thick	0.6	$2.3(5)\cdot10^{-6}$	66(2)
316L_Cu_very_thick	0.65	$1.3(5)\cdot10^{-6}$	63(2)
316L [4]	0.5	$8(1)\cdot10^{-7}$	58(1)

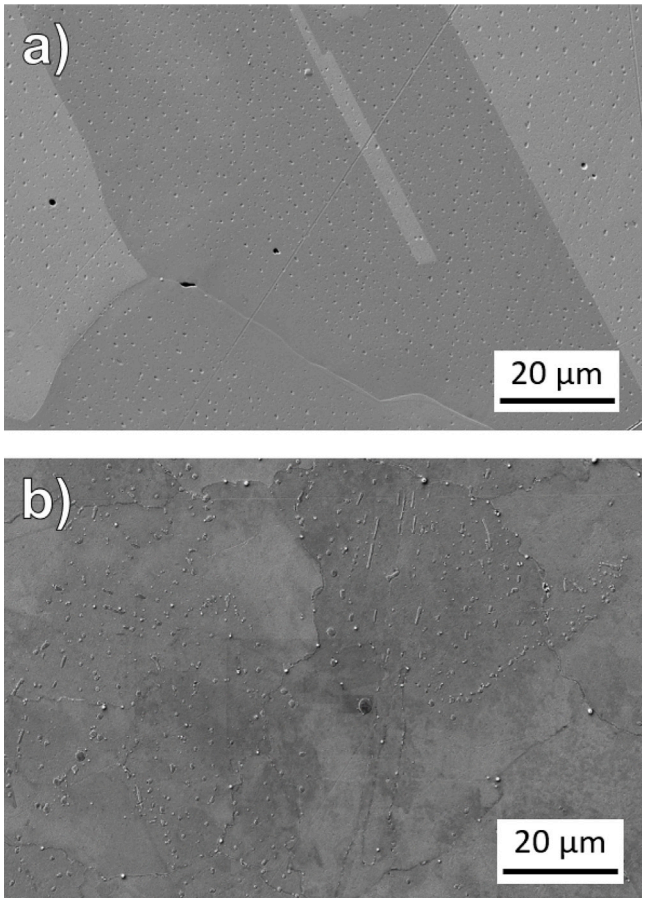

Fig. 2. SEM images of the polished surfaces: a) Cu; b) CuCrZr.

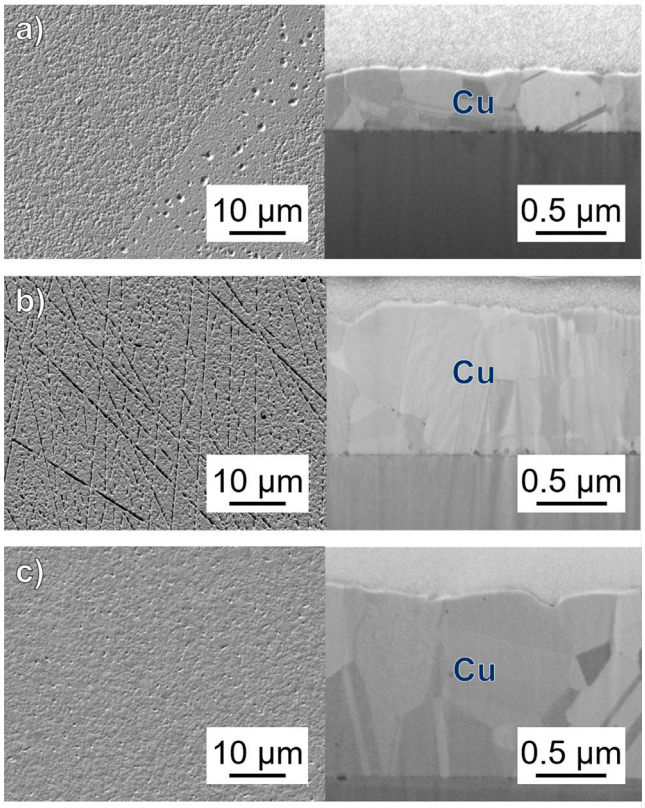

Fig. 3. Left: SEM figures of the surface; Right: SEM figures on the cross sections prepared by FIB of the coated substrates: a) 316L_Cu_thin; b) 316L_Cu_thick; c) 316L_Cu_very_thick. On top of the Cu layer, a Pd layer is visible. The Pd layer was applied for the FIB cut in order to avoid surface damage and the curtaining effect during FIB cut.

given in Table 1. The same analysis was performed on all samples and the results are given in Table 1. The values are valid in the measured temperature (300°C to 550°C) and pressure (25 mbar to 800 mbar) ranges. Since the up- and down-measurements corresponds to each other, no change of sample during measurement is observed. The data for the 316L substrate were taken from the publication [4] and will be used for the calculation of the Cu layer permeability. The permeabilities versus sample temperature of all samples listed in Table 1 are shown in Fig. 5.

The layer permeabilities of all Cu layers are calculated according to Eq. (2). For the substrate permeability, the values for 316L are used. For the layered substrate permeability, the values for 316L_Cu_thin, 316L_Cu_thick, and 316L_Cu_very_thick are taken from Table 1. The layer permeabilities can be found in Table 2 and are plotted in Fig. 6.

6. Discussion

The permeabilites of the Cu and the CuCrZr samples are very similar and P_0 and E_P of CuCrZr are within the error bars of the values for Cu (Table 1). From this it is concluded that the precipitates do not influences the permeability and that the permeability is mainly defined by the Cu matrix. In both cases, the diffusion is limiting the permeation process. The measured value for the Cu sample are in agreement to the adapted literature value for deuterium permeation through copper [7].

In the Cu layered substrates the permeation process is mainly limited by the diffusion process, see Table 1. A reduction of the permeability of the 316L_Cu samples is expected due to the coating in comparison to the uncoated substrate, since Cu shows a lower permeability than 316L. The expected permeability of the 316L_Cu_very_thick sample was calculated with Eq. (2) by using the permeabilities of Cu bulk and 316L

Table 2
The layer permeabilities calculated according Eq. (2). The mean value (MV) of the Cu layers is calculated from the permeabilites of the three Cu layer permeabilites, see text.

Layer	P_0 $\left[\frac{\text{mol}}{\text{ms}\sqrt{\text{mbar}}}\right]$	E_P $\left[\frac{\text{kJ}}{\text{mol}}\right]$
Cu_thin Layer	$3{\cdot}10^{-10}$	42
Cu_thick Layer	$2{\cdot}10^{-6}$	93
Cu_very_thick Layer	$3{\cdot}10^{-7}$	80
MV Cu Layer	$7{\cdot}10^{-8}$	72

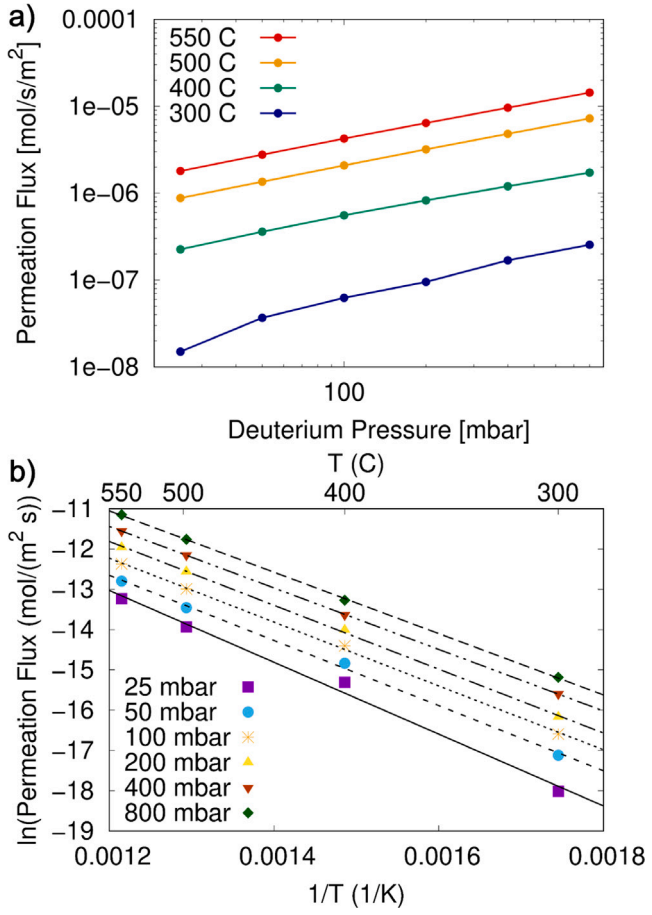

Fig. 4. a) Stabilized permeation flux through the 316L_Cu_thick sample versus the applied deuterium pressure. The colors indicate the sample temperatures. b) The corresponding Arrhenius plot for the 316L_Cu_thick sample. The lines represent the fitted lines to the data in order to obtain E_P and P_0, see Table 1. The color points represent the measurement points at different applied deuterium pressures. (For interpretation of the references to color in this figure legend, the reader is referred to the web version of this article.)

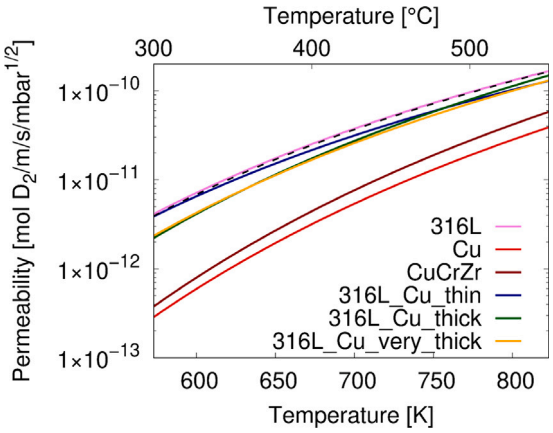

Fig. 5. Permeability versus sample temperature for Cu, CuCrZr and the Cu layered 316L substrates with the values from Table 1. The permeability for the 316L substrate is taken from [4]. The black dotted line is the estimated permeability for the 316L_Cu_very_thick sample by using the Cu bulk value, see text.

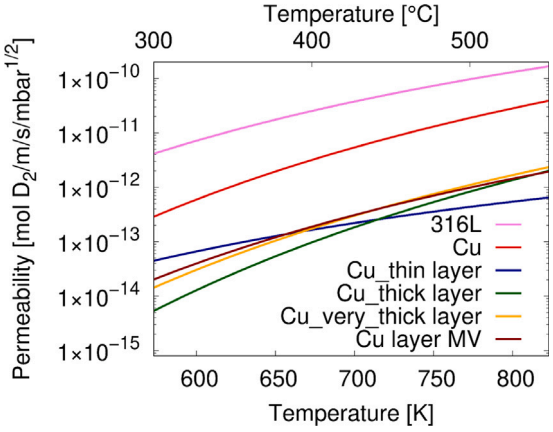

Fig. 6. Permeability versus sample temperature for the Cu layers from Table 2 and for comparison of the bulk Cu and 316L substrates. The mean value (MV) of the Cu layers are calculated from the permeabilites of the three Cu layer permeabilites, see text.

from Table 1. The expected reduction is very small and the calculated result is shown as a black dotted line in Fig. 5. Comparing the expected permeability with the measured permeability of the 316L_Cu_very_thick sample, the measured permeability is lower than expected. By calculating the Cu layer permeability the difference can be seen in Fig. 6. The permeability of the Cu layer is about one order of magnitude lower as the bulk Cu permeability.

As explained above, the layer permeability contains all sample characteristics, such as effects of interfaces, microstructure and surface effects. In order to study whether the interface is the reason for the reduced Cu layer permeability or any other effect, the layer thickness was varied as explained above and illustrated in Fig. 1: The Cu layer permeability contains the permeability of the layer bulk (P_{LB}) and the interface (P_{int}). By varying the layer thickness, the layer bulk and interface ratio is varied and the influence of the interface and the bulk (microstructure) can be separated. If the microstructure is the reason for the difference compared to the Cu bulk sample, the permeability of the Cu layer is diffusion limited and the permeabilities of the layered substrates (P_{tot}) scale with the thicknesses of the layer. Furthermore, Eq. (2) would be valid and the layer permeability of all Cu layers would be the same. In the opposite case, in which the influence of the interface plays the major role for the difference, the layered substrate permeability should be very similar in all layered substrates and independent of the layer thickness. Eq. (2) would not be valid which would lead to an increase of the calculated layer permeability with increasing the layer thickness.

From the layered substrate permeabilities in Fig. 5 and Table 1 no clear behavior can be extracted. There is a difference between all layered substrate permeabilities and since the P_0 and E_P are very

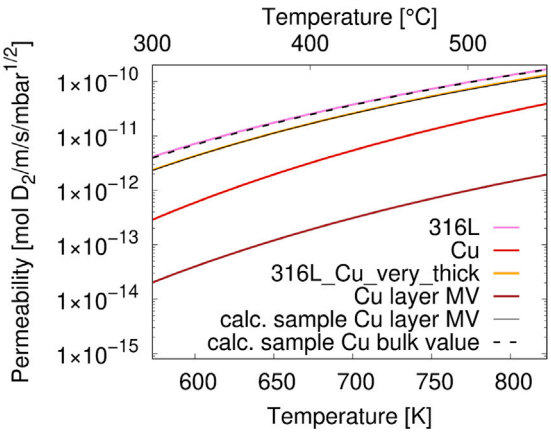

Fig. 7. The 316L_Cu_very_thick sample permeability (black line) calculated with the Cu Layer MV (brown line). For comparison, the Cu bulk (red line), the 316L substrate (violet line), the calculated 316L_Cu_very_thick sample with the Cu bulk value (black dotted line), and the measured 316L_Cu_very_thick sample (yellow line) permeabilities are shown. (For interpretation of the references to color in this figure legend, the reader is referred to the web version of this article.)

different, the slope of the curves are different as well. The differences in slope can be observed in the layer permeabilities as well, see Fig. 6 and Table 2. Nevertheless, since the layer permeabilities are all in the same order of magnitude, the conclusion is that the microstructure is the major reason for the larger reduction of the layer permeability compared to the Cu bulk sample. Since the pressure dependence is only slightly increased in the layered substrates, see Table 1, the diffusion is mainly limiting the permeation process. This is a second confirmation that the interface do not have a significant influence on the permeation flux in this case.

A mean value (MV) was calculated from all three Cu layer permeabilites, see Table 2 and the brown curve in Fig. 6. From this Cu Layer MV the layered substrate permeability was calculated for the 316L_Cu_very_thick sample, see black line in Fig. 7. As a summary, a comparison is shown in this figure between the Cu bulk, the Cu layer MV, the calculated 316L_Cu_very_thick sample with the Cu bulk value (black dotted line) and the measured 316L_Cu_very_thick sample permeability. The conclusion is that there might be an influence of the interface on the permeation, but in this case the influence of the microstructure on the permeation is much larger and the major reason for the reduction.

7. Conclusions

In both polished Cu and CuCrZr samples, diffusion is limiting the permeation process. The permeabilities of Cu and CuCrZr are similar and in agreement with literature data for Cu.

The measured reduction of the 316L permeability due to the Cu coating is much larger than expected from an estimation using the Cu bulk permeability. By varying the layer thickness, the layer bulk and interface ratio was changed and the influence of the microstructure and the interface on the permeability could be separated. The conclusion is, that the influence of the microstructure is the major reason for the reduction and the influence of the interface on the permeability is minor is this case. The Cu layer permeability is about one order of magnitude smaller as the Cu bulk permeability. Further material combinations, e.g., W on CuCrZr, are under study.

CRediT authorship contribution statement

A. Houben: Conceptualization, Methodology, Formal analysis, Investigation, Writing – original draft, Visualization, Project administration. **M. Rasiński:** Formal analysis, Investigation. **S. Brezinsek:** Conceptualization, Resources, Writing – review & editing. **Ch. Linsmeier:** Conceptualization, Resources, Writing – review & editing, Funding acquisition.

Declaration of competing interest

The authors declare that they have no known competing financial interests or personal relationships that could have appeared to influence the work reported in this paper.

Data availability

Data will be made available on request.

Acknowledgments

The authors thank G. De Temmerman (ITER Oranisation) and S. Heikkinen (F4E) for providing the CuCrZr-IG sample material and B. Göths for sample preparation.

This work has been carried out within the framework of the EUROfusion Consortium, funded by the European Union via the Euratom Research and Training Programme (Grant Agreement No 101052200 — EUROfusion and 2019–2020 under grant agreement No 633053). Views and opinions expressed are however those of the author(s) only and do not necessarily reflect those of the European Union or the European Commission. Neither the European Union nor the European Commission can be held responsible for them.

References

[1] R. Causey, Hydrogen isotope retention and recycling in fusion reactor plasma-facing components, J. Nucl. Mater. 300 (2–3) (2002) 91–117.
[2] K. Ioki, P. Barabaschi, V. Barabash, S. Chiocchio, W. Daenner, F. Elio, M. Enoeda, A. Gervash, C. Ibbott, L. Jones, V. Krylov, T. Kuroda, P. Lorenzetto, E. Martin, I. Mazul, M. Merola, M. Nakahira, V. Rozov, Y. Strebkov, S. Suzuki, V. Tanchuk, R. Tivey, Y. Utin, M. Yamada, Design improvements and R&D achievements for vacuum vessel and in-vessel components towards ITER construction, Nucl. Fusion 43 (4) (2003) 268–273.
[3] M. Li, S.J. Zinkle, Physical and mechanical properties of copper and copper alloys, in: R. Konings (Ed.), Comprehensive Nuclear Materials, Vol 4: Radiation Effects in Structural and Functional Materials for Fission and Fusion Reactors, 2012, pp. 667–690.
[4] A. Houben, J. Engels, M. Rasiński, C. Linsmeier, Comparison of the hydrogen permeation through fusion relevant steels and the influence of oxidized and rough surfaces, Nucl. Mater. Energy 19 (2019) 55–58.
[5] A. Houben, M. Rasinski, C. Linsmeier, Hydrogen permeation in fusion materials and the development of tritium permeation barriers, Plasma Fusion Res. 15 (1) (2020).
[6] P. Ostachowski, W. Bochniak, M. Lagoda, S. Ziolkiewicz, Strength properties and structure of CuCrZr alloy subjected to low-temperature KOBO extrusion and heat treatment, Int. J. Adv. Manuf. Technol. 105 (12, SI) (2019) 5023–5044.
[7] R. Causey, R. Karnesky, C.S. Marchi, 4.16 - Tritium barriers and tritium diffusion in fusion reactors, in: R.J. Konings (Ed.), Comprehensive Nuclear Materials, Elsevier, Oxford, 2012, pp. 511–549.